2023

Diffusion of Carbon Nanoparticles Intercalated into Layered Materials

Madelyn Johnson
University of Northern Iowa

DIFFUSION OF CARBON NANOPARTICLES INTERCALATED INTO LAYERED MATERIALS

A Thesis Submitted

in Partial Fulfillment

of the Requirements for the Designation

University Honors

Madelyn Johnson

University of Northern Iowa

May 2023

This Study by: Madelyn Johnson

Entitled: Diffusion of Carbon Nanoparticles Intercalated into Layered Materials

has been approved as meeting the thesis of project requirement for the Designation University Honors

_____	_____
Date	Dr. Tim Kidd, Honors Thesis Advisor, Department of Physics
_____	_____
Date	Dr. Jessica Moon, Director, University Honors Program

Abstract

Using electron beam radiation, as found in a scanning electron microscope, it is possible to induce the local intercalation of carbon nanoparticles into two dimensional layered materials. This technique can be used to form insulating and optically active nanostructures in samples ranging from graphite to BSSCO. In this study, the evolution of these features with time is explored to determine the stability of such nanoparticles in layered materials.

Over the course of days and weeks, the nanostructures created this way broaden and change height. In general, it appears that material buried deep within the layers diffuses upwards to increase the height of the material observed at the surface. The process proceeds rapidly in defective crystal structures like titanium disulfide (TiS_2) and slowly in rigid oxides like BSSCO. The carbon nanoparticles within TiS_2 diffused laterally and grew in height. The surface roughness of TiS_2 also increased as time progressed. The carbon nanoparticles intercalated into BSSCO did not diffuse significantly and the surface roughness remained constant throughout the observation period.

This work is important in determining the overall stability of these structures and their utility to form nanoscale devices like Josephson tunnel junctions. Understanding how carbon nanoparticles behave in these layered materials can provide useful insights to how other materials would behave within the layered material.

Table of Contents

Chapter 1. Introduction

Dichalcogenides are layered materials. They are comprised of a transition metal and two chalcogens. The transition metal sits between two layers of chalcogen, with each metal ion sharing bonds with three chalcogens above and three chalcogens below. Figure 1.1 shows a transition metal, represented in black, and two layers of chalcogen, represented in yellow, forming hexagonal layers weakly connected by van der Waals forces. These transition metal dichalcogenides have weak van der Waals bonding between layers and stronger intra-place covalent bonding. These dichalcogenides have been researched for utilization in things like Josephson tunnel junctions, photovoltaic devices, lithium-ion batteries, transistors, and memory devices (Lv et al., 2015).

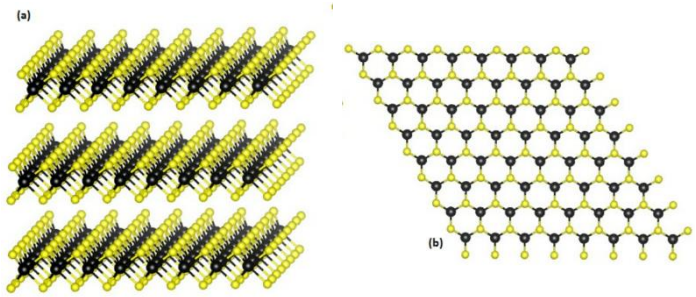

Figure 1.1 – Image (a) displays a side view of layers of a dichalcogenide, the transition metal (M) represented in black and the chalcogen (X) represented in yellow. Van der Waals gaps can be seen between the MX_2 layers. Image (b) displays the top view, where the crystal structure can be visualized. ("Transition Metal Dichalcogenide Monolayers," 2023)

Intercalation is the process by which foreign materials are introduced into the van der Waals gap of a crystal structure. Figure 1.2 shows a guest species intercalating between two layers of a material.

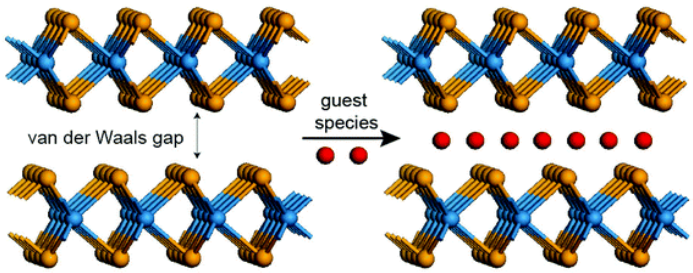

Figure 1.2 – This figure shows how a guest species intercalates into the van der Waals gap of a layered material (Jung et al., 2016).

Electron beam (EB) lithography is the process in which a sample is exposed to a concentrated beam of electrons. This can write patterns onto the surface, and regarding dichalcogenides, stimulates intercalation of carbon nanoparticles. This can be done using different techniques, but to prepare the samples used in this project, a scanning tunneling microscope (SEM) was used.

The SEM provides a beam of high energy electrons. These electrons excite residual organic molecules on the surface, which ionizes them. This ionized organic material then diffuses into the layered material.

An atomic force microscope (AFM) was used to image the samples over a period of time. An AFM can produce topography and phase images. Topography images show differences in height on the sample while phase images show differences in chemical composition of the sample. Figure 1.3 shows a simplified diagram of an AFM. The tip runs along the surface of the sample, compensating for changes on the sample. This compensation moves the cantilever which in turn moves the reflected laser on the photodiode. This then creates a contour map on the photodiode.

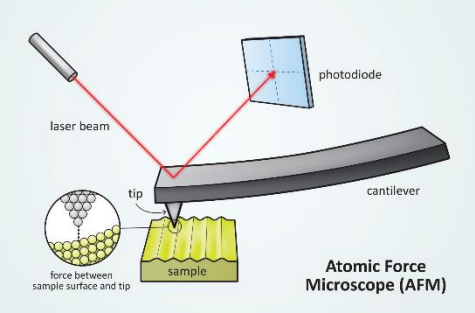

Figure 1.3 – This image shows the set-up of an atomic force microscope (*Scientific Image - Atomic Force Microscope Illustration | NISE Network*, n.d.)

An SEM was used by the researchers Kidd et al. to measure and synthesize nanostructures within layered materials, and discovered the process was universal for layered materials. In their research, they noticed a "halo" effect, most easily seen in AFM phase images taken of the samples. They concluded that the e-beam radiation used to create the nanostructures could affect surrounding areas and expand past the initially set region of exposure. They stated they believed it was most likely due to electron scattering within the sample and residual organics on the sample, causing the formation of nanostructures outside the designated region.

Rykaczewski et al. performed e-beam-induced carbon deposition studies with very similar conditions and parameters to form nanopillars with associated rings and saw a similar halo effect. Electron beam induced dissociation (EBID) of hydrocarbons is a consequence of e-beam exposure. EBID leaves carbon behind on the surface, somewhat burning the sample, allowing for the creation of carbon-based organic nanostructures within the layered material. One key difference between the two results was that Rykazcewki et al. found a quicker nanostructure formation rate, orders of magnitude faster. In their experiments they monitored the height of the associated ring as well as the nanopillar to find the relationship between the two heights during the exposure process.

While an interesting link certainly exists between this work and Kidd et al's study, Kidd et al. concluded that they should have been able to detect nanostructures on non-layered materials with an optical microscope if the only difference between the two works was the enhanced deposition rates from a larger existence of residual organics in the system. Rykaczewski et al. confirmed that residual organic matter and backscattered electrons can cause problems in electron microscopy but were unable to provide a relationship between the nanostructure formation and

time, during and after exposure. Kidd et al. reported in their study that density held an important role in nanostructure formation. Lower density led to smaller heights in the structures and wider halos, especially in graphite.

Since its publication in 2014, Kidd et al.'s work has been used to investigate electron beam induced reduction of graphite oxide by in situ X-ray photoelectron spectroscopy by Zhu et al. at the Institute of Chemical Materials, China Academy of Engineering Physics. It was also used to further explore the manipulation of subsurface carbon nanoparticles in $Bi_2Sr_2CaCu_2O_{8+\delta}$ using a scanning tunneling microscope by Stollenwerk et al. at the University of Northern Iowa. Neither of these studies focused on looking further into the properties of the nanostructures formed by residual organics and backscattered electrons nor the diffusion of nanostructures over time, which is why this study is important to better understand the properties of these nanostructures.

Investigating the relationship between the diffusion of nanoparticles in layered materials and time is important in better understanding these nanoparticles and the materials overall stability. By understanding how material diffuses along and through the layers, information about the material can be learned and then applied to create nanoscale devices.

Chapter 2. Methods

The TiS_2 samples were synthesized by Tyler Rash, Laura Strauss, and Tim Kidd of the University of Northern Iowa, and the BSSCO samples were synthesized by Genda Gu of the Brookhaven National Laboratory. After synthetization, the samples were exposed to e-beam radiation which induced the intercalation of carbon nanoparticles.

Two types of samples were created. In filled box samples, the exposed region was a filled square. In an empty box sample, the exposed region was an outline of a square.

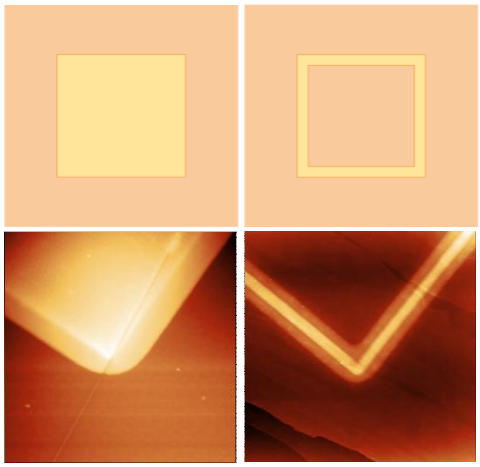

Figure 2.1 – Cartoon representations of the two types of samples: filled box (top left) and empty box (top right) can be compared to the topography images of a filled box sample (bottom left) and an empty box sample (bottom right).

AFM images were obtained by Amber Hartness over a period of months to evaluate the diffusion of nanoparticles. The samples were untouched between AFM images. This project focused on analyzing the AFM images taken in 2015. A description of the methods for this image analysis is described in Chapter 3.

Chapter 3. Image Analysis

The AFM images were opened in Gwyddion (Nečas et al., n.d.), a software for visualization and analysis of data. The analysis described below was done using topography images. A yellow-rust color gradient was added to the image. Depending on the quality of the image, one or more of the following Gwyddion features were used to prepare the image for analysis: level data by mean plane subtraction, remove polynomial background, stretch color range to part of data, and shift minimum data value to zero. Using these four features, the image background was flattened, the colors were adjusted, and the data was zeroed.

Profiles were drawn across the exposed region of the sample with a set profile width of three pixels. After drawing three to four profiles, a height plot including each profile was created within Gwyddion.

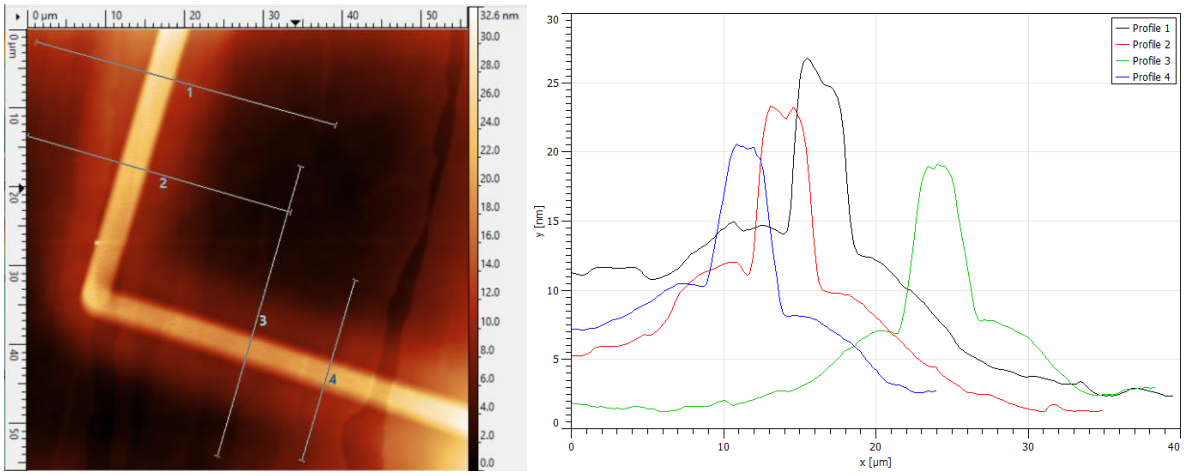

Figure 3.1 – The left image shows the profiles drawn perpendicular to the exposed region on a TiS_2 Day 3 topography image. The right image shows the associated height plots for each drawn profile in the left image.

The data for each profile was then exported to Origin for further analysis. To do this, the data was first transferred to Microsoft Excel where the position values were converted from meters to micrometers and the height values were converted from meters to nanometers.

To graph the profile data in Origin, the column of x values and associated y values were selected and plotted on the Scatter setting. Each plot had a background, which needed to be removed for a more accurate analysis. This background is any data in the graph that is not a part of the peaks. To do this in Origin, points considered to be background data were selected. After

selecting the points, the interpolation method was determined based on which looked best and interfered with the peak data the least.

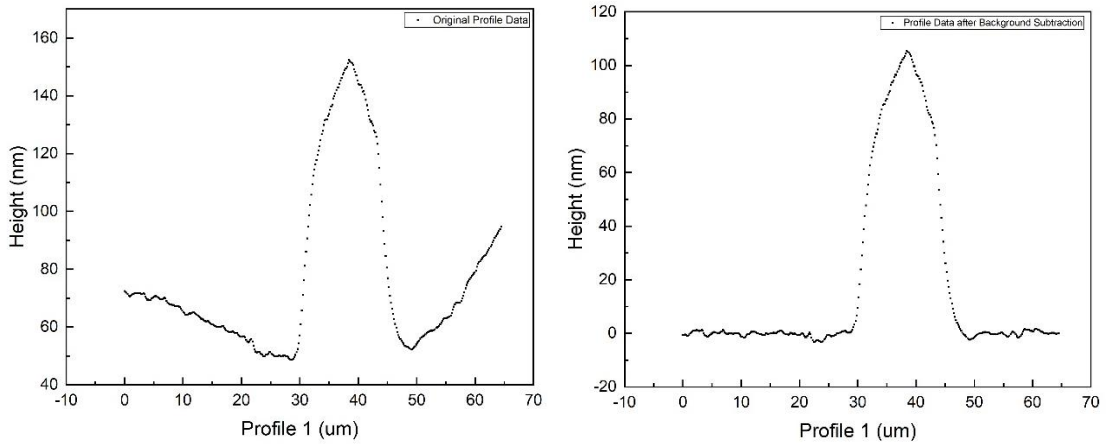

Figure 3.2 – The left graph shows TiS_2 Day 90 profile data. The right graph shows the same Day 90 profile data after background subtraction.

After subtracting the background, the modified data was replotted, and the range of the plot was modified to only include the peaks. This graph was then used for the further analysis described below.

To fit the data, a fitting function was created using the Fitting Function Builder in Origin. The full equation is presented below:

$$y(x) = \frac{I_1\alpha_1}{\delta_1\sqrt{2\pi}} * e^{-\frac{1}{2}\left(\frac{x-(x_c+dx_1)}{\delta_1}\right)^2} + \frac{I_1}{\delta_1\sqrt{2\pi}} * e^{-\frac{1}{2}\left(\frac{x-(x_c-dx_1)}{\delta_1}\right)^2} + \frac{I_2\alpha_2}{\delta_2\sqrt{2\pi}} * e^{-\frac{1}{2}\left(\frac{x-(x_c+dx_2)}{\delta_2}\right)^2} + \frac{I_2}{\delta_2\sqrt{2\pi}} * e^{-\frac{1}{2}\left(\frac{x-(x_c-dx_2)}{\delta_2}\right)^2} \quad \text{(Eq – 3.1)}$$

The first two terms are associated with the two center peaks and the last two terms are associated with the two outer peaks. The *I* values are intensity values and affect the amplitude of the peaks. The α values also affect amplitude and create an offset between the two symmetrical peaks. The δ values are the standard deviation and are associated with the width of the peaks. The x_c value represents the position of the center of the peak. For this data, the x_c value represents the center of the fit. The *dx* values represent the distance of the center of the peak from the x_c value.

Origin's curve fitting function was used to fit the data, selecting Equation 3.1 as the fit equation. A preview of the fit, with the arbitrary initial parameters, was plotted on top of the data. The values of each parameter were changed slightly to find a better fit. Once the fit looked close to correctly fitting the data, the Fit button was pressed. Starting from the estimated parameters, Origin updated the parameters until the fit converged and the minimum Chi-squared value was

reached. The fit parameters were put into a table and added to the graph window. These parameters were recorded in a spreadsheet for future analysis.

Surface roughness was also used for analysis, and Gwyddion was used to determine this surface roughness. To quantitatively look at the surface roughness, root mean square (RMS) was used. To determine this, the image was rotated and cropped to select a section of the topography image to analyze.

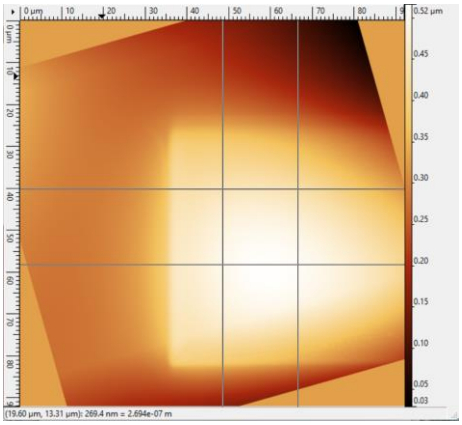

Figure 3.4 – This figure shows a topography image of the Day 5 TiS_2 filled box in Gwyddion with a section selected for cropping.

The background was removed from the cropped image using the plane subtraction and/or the polynomial subtraction. From here, the moment-based RMS (σ) calculated by Gwyddion, was recorded. The equation used by Gwyddion is shown below:

$$\sigma = \mu_2^{1/2}; \qquad \mu_i = \frac{1}{N}\sum_{n=1}^{N}(z_n - \bar{z})^i \qquad \text{(Eq – 3.2)}$$

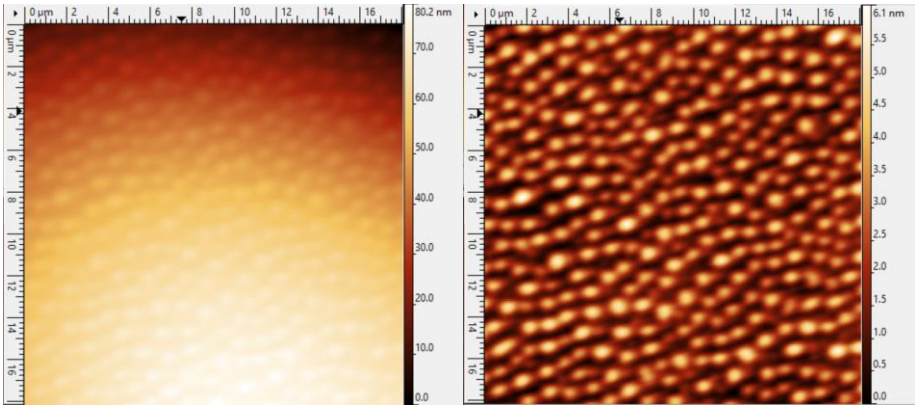

Figure 3.5 – This figure shows the cropped image of Day 5 TiS_2 filled box exposed surface from Figure 3.4 before (left) and after (right) second degree polynomial background removal.

To qualitatively look at surface roughness, profiles were drawn across small regions of topography images of both filled and empty box samples. The height profiles were used to make conclusions about the nature of the material at the surface.

Chapter 4. Analysis of Diffusion and Narrow Features

Two materials were analyzed: Titanium disulfide (TiS_2), and Bismuth strontium calcium copper oxide (BSSCO).

$\underline{TiS_2}$:

To monitor the movement of carbon nanoparticles within the sample over time, profiles across the exposed region of the sample were fitted with Equation 3.1, as described in Chapter 3. The parameters of the fit were graphed over time to better understand the evolution of the nanoparticles.

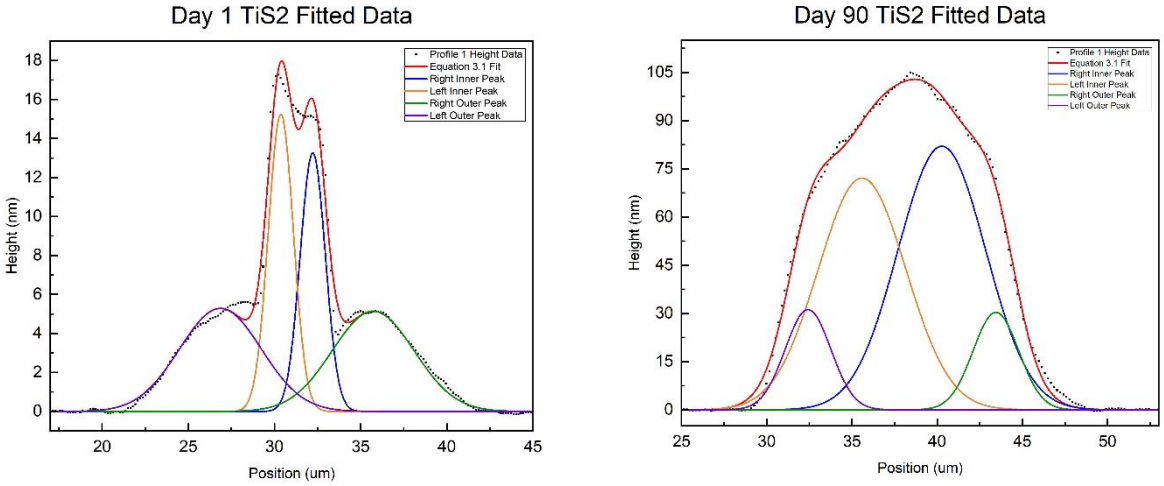

Figure 4.1 – The plots include the data and Equation 3.1 fit (red) for a profile on the initial date of observation (left) and for the last date of observation (right) for the TiS_2 sample. The breakdown of the Equation 3.1 fit can be understood by the individual peaks included in the graphs (purple, orange, blue, and green).

In Figure 4.1 the fit from the initial date (6/26/15) and the fit from the final date (9/24/15) show the drastic increase in height for both inner and outer peaks after 90 days. This increase in height is predicted to be due to the movement of the material initially buried within the layers moving towards the surface.

Using the parameter values given by the Equation 3.1 fit in Origin, plots of average peak height and total area were created as a function of time. Peak height can be extracted from the fit when x is equal to xc ± dx. This would make the exponent term in the equation to be equal to 1, leaving only $\frac{I\alpha}{\delta\sqrt{2\pi}}$ and $\frac{I}{\delta\sqrt{2\pi}}$. Therefore, average peak height for a given day was determined using Equation 4.1.

$$Average\ Peak\ Height = \frac{1}{2}\left[\frac{I\alpha}{\delta\sqrt{2\pi}} + \frac{I}{\delta\sqrt{2\pi}}\right] \qquad \text{(Eq - 4.1)}$$

Equation 4.1 was applied to both the inner and outer peaks, and both plots can be found in Figure 4.2.

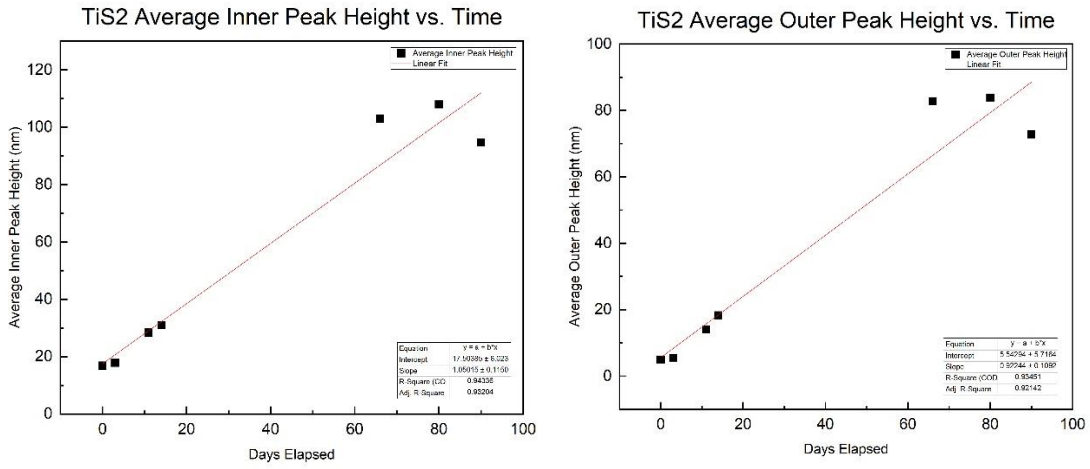

Figure 4.2 – The inner peak height vs. time (left) and the outer peak height vs. time (right) for TiS_2 both grow linearly and are fit with a linear function (red).

Figure 4.2 shows that both the inner and outer peaks grow linearly with time. The slopes of the two graphs are also similar, which suggests that they grow at a similar rate.

Total area can be used to determine if the nanoparticles on the surface are growing in height, or if the nanoparticles are simply moving. Total area was calculated using Equation 4.2.

$$Total\ Area = I_1 + (I_1 * \alpha_1) + I_2 + (I_2 * \alpha_2) \qquad \text{(Eq – 4.2)}$$

Ideally, individual peak area would allow more thorough conclusions to be made about the diffusion and growth of nanoparticles in this system, but due to the proximity of the peaks to one another, their parameters are inter-dependent.

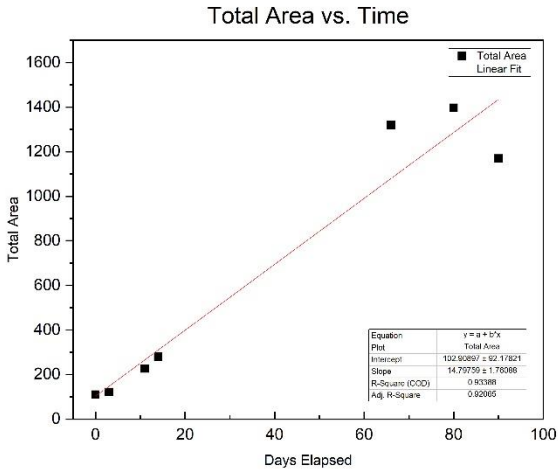

Figure 4.3 – Total area calculated using Equation 4.2 for TiS_2 is plotted vs. time in this figure. A linear fit (red) was added to the plot as it appears that total area increases linearly.

Figure 4.3 shows that total area increases linearly as a function of time. This increase in total area suggests that there is aggregation of nanomaterial at the surface, not solely a redistribution of the material. The total area grows in a similar relationship with time as peak height grows with time which indicates that the aggregation of material lends mostly to an increase in height, as opposed to lateral diffusion.

BSSCO

After observing an exposed region of a filled box on BSSCO for 145 days, little change was observed. Profiles were taken from inside the exposed region, through the edge of the box, and into the background, as shown in Figure 4.4.

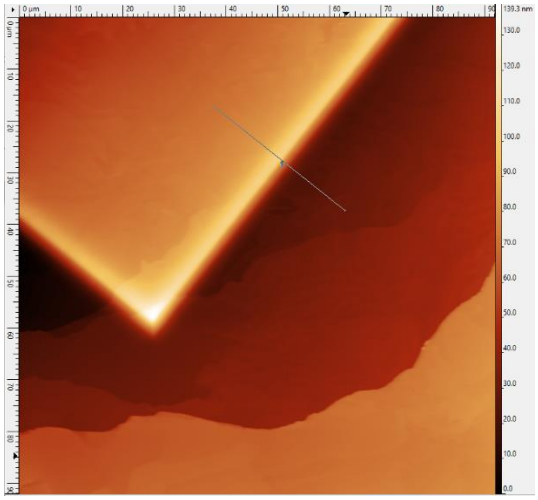

Figure 4.4 – A profile taken across the edge of a topography image of a filled sample of BSSCO

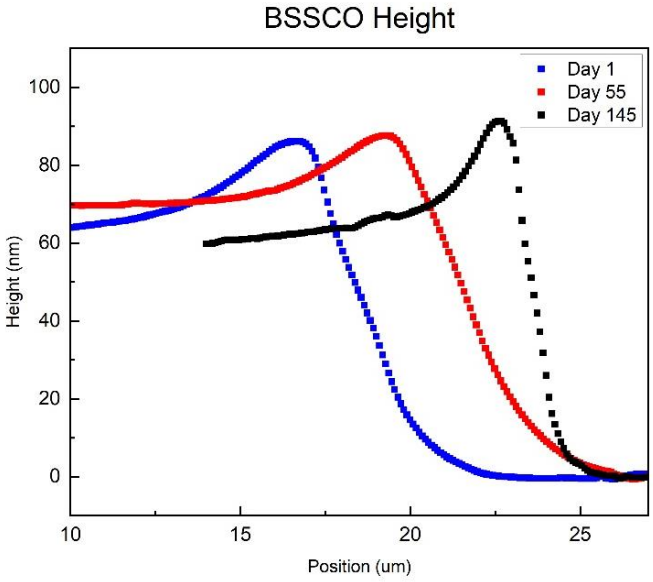

Figure 4.5 – Three profiles taken from the same BSSCO sample on different days: 7/8/15 (blue), 9/1/15 (red), and 11/30/15 (black).

Figure 4.5 shows profiles taken on three different days, one at the beginning of the period, one at the middle of the period, and one at the end of the period. Comparing the three profiles, it is evident that the BSSCO experiences a much less drastic growth compared to the TiS_2. Due to this limited growth, further analysis was not conducted at this time.

Chapter 5. Surface Roughness

Surface roughness gives insight to the quality of the surface of the sample. Comparing AFM images of the TiS_2 sample allows for the qualitative analysis of the surface roughness.

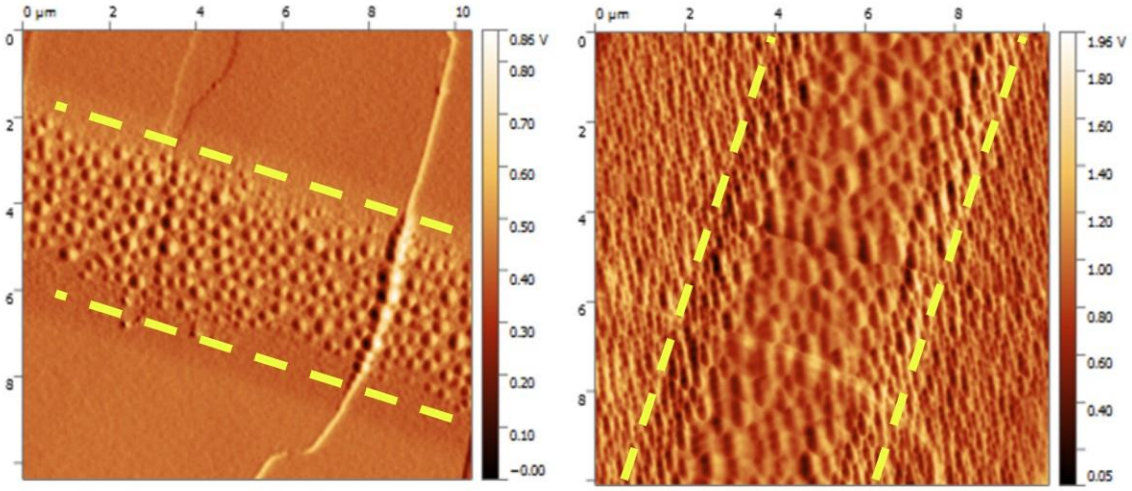

Figure 5.1 – Enlarged AFM topography images of the empty box TiS_2 sample where the initially exposed region is outlined with yellow dashed lines. The left image was taken 4 days after the initial exposure and the right image was taken 66 days after the initial exposure.

Surface roughness can be due to nanostructures irritating the surface or surface oxidation. Figure 5.1 clearly shows the increase in surface roughness of the TiS_2 sample.

Surface roughness of the TiS_2 sample was measured qualitatively by comparing height profiles taken on three regions. Figure 5.2 shows the analysis for Day 1.

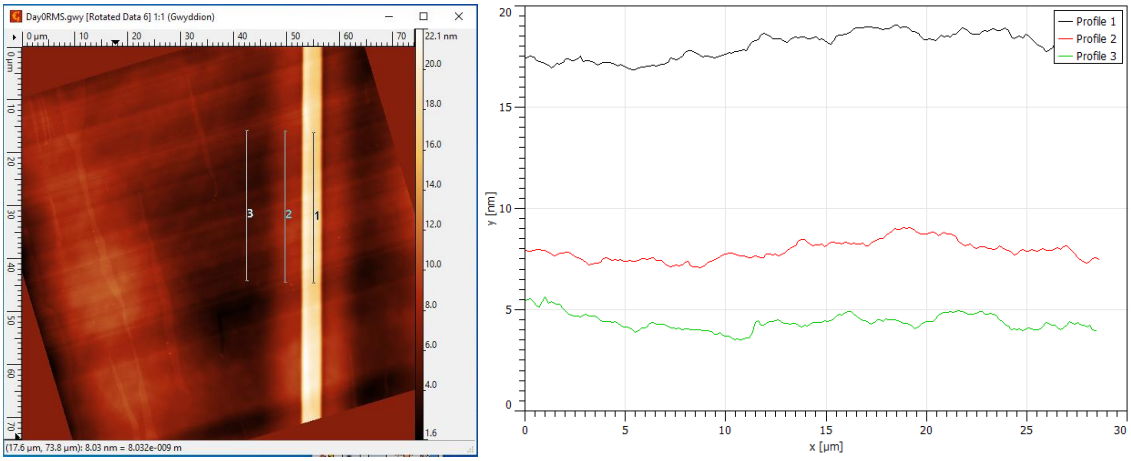

Figure 5.2 – The left image shows profiles taken on day 1 on the exposed region, halo region, and background on the TiS_2 topography image. The graphed heights for each profile are shown in the right image.

By looking at the shapes of each plotted profile, it is evident that the profiles in all three regions produce relatively flat profiles, which indicates little change in height.

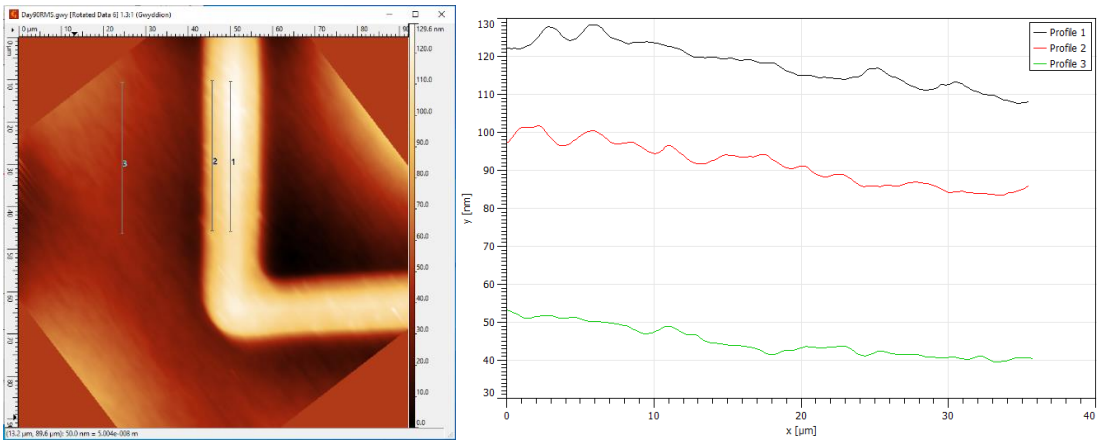

Figure 5.3 – The left image shows profiles taken on day 90 on the exposed region, halo region, and background on the TiS_2 topography image. The graphed heights for each profile are shown in the right image.

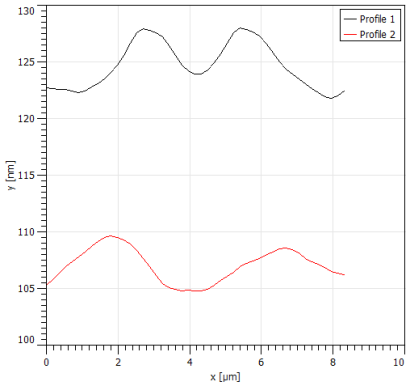

Figure 5.4 – An enlarged version of the graph in Figure 5.3.

The Figure 5.3 plotted profile in the background region (profile 3) remains relatively flat while the profiles of the two exposed regions include visible peaks.

Figure 5.4 shows that there are defined peaks in the graphed profile which indicates there are piles of material on the surface in the exposed region.

To monitor the evolution of these piles of material on the surface, Gwyddion was used to measure the size of the piles on filled box samples of the TiS_2.

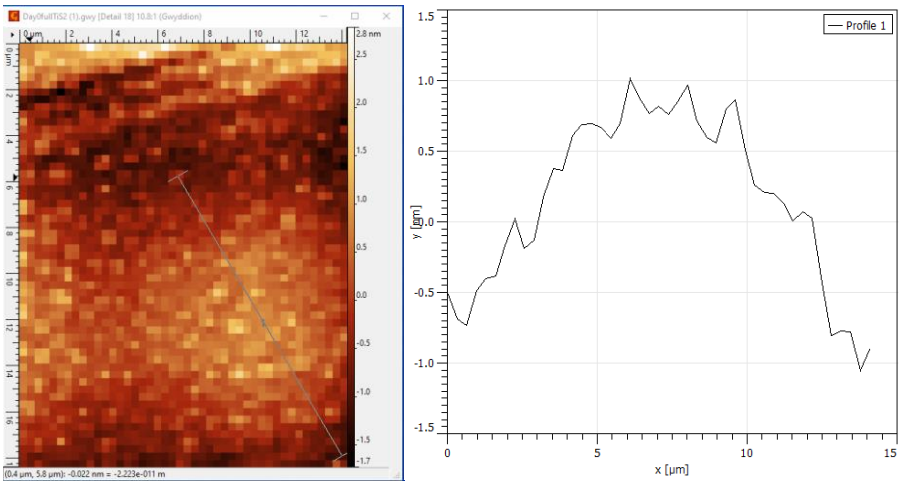

Figure 5.5 – A profile taken across a pile identified on the exposed region of an enlarged image of the TiS_2 filled sample on day 1 (left) produces a height graph (right) of the pile.

The height graph in Figure 5.5 shows the pile on the exposed region of the TiS_2 sample is roughly 1.0 nm tall. Over time, the observed piles on the exposed region gradually grew in height.

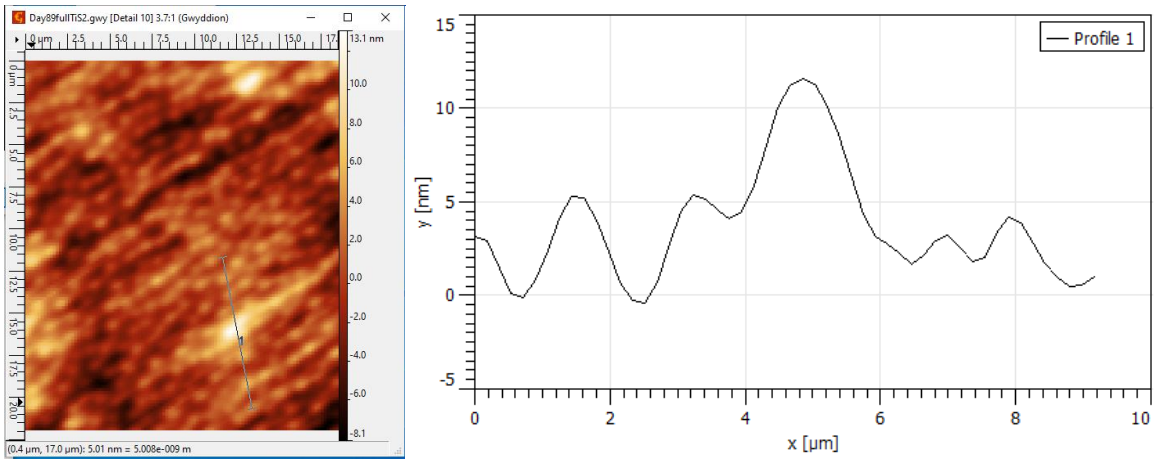

Figure 5.6 – A profile taken across a pile identified on the exposed region of an enlarged image of the TiS_2 filled sample on day 90 (left) produces a height graph (right) of the pile.

Figure 5.6 shows the piles on the exposed region of the TiS_2 sample are roughly between 5.0 and 12.0 nm tall. Compared to Day 1 in Figure 5.5, this shows significant growth of these piles on the exposed surface.

Surface roughness of the TiS_2 sample was measured quantitatively using Gwyddion with the method outlined in Chapter 3. RMS surface roughness was measured inside and outside the exposed region of a filled TiS_2 sample.

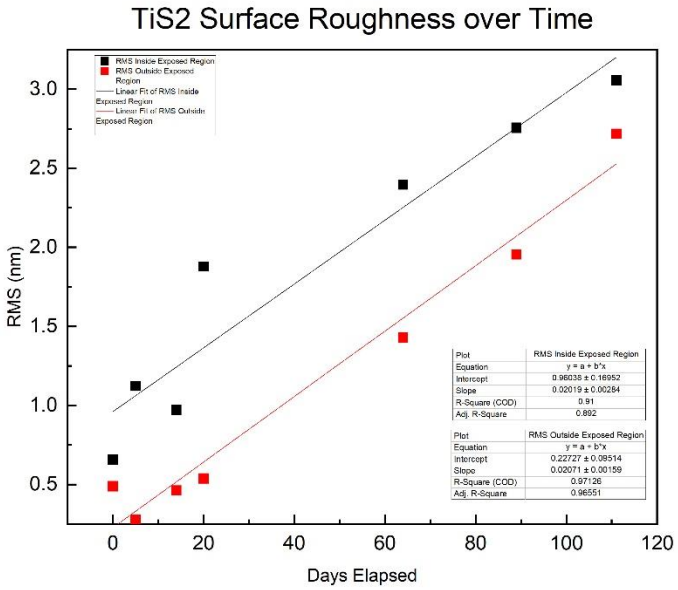

Figure 5.7 – This plot includes data for surface roughness on the exposed region (black) and on the background region (red). The slope of the exposed region fit is 0.0202 nm/day and the slope of the background region fit is 0.0207 nm/day.

The RMS surface roughness on the exposed region and on the background region increases with time. The linear fit applied to both sets of data in Figure 5.7 have similar slopes which indicates that the surface roughness on both regions increases at a similar rate. The increase in the background region is most likely solely due to oxidation on the surface. The piles on the exposed region are growing in height, which would account for the increase on this region, along with surface oxidation.

The surface roughness on a filled sample of BSSCO was also monitored over time. Over the 145 days of observation, surface roughness on the exposed region and background remained relatively constant.

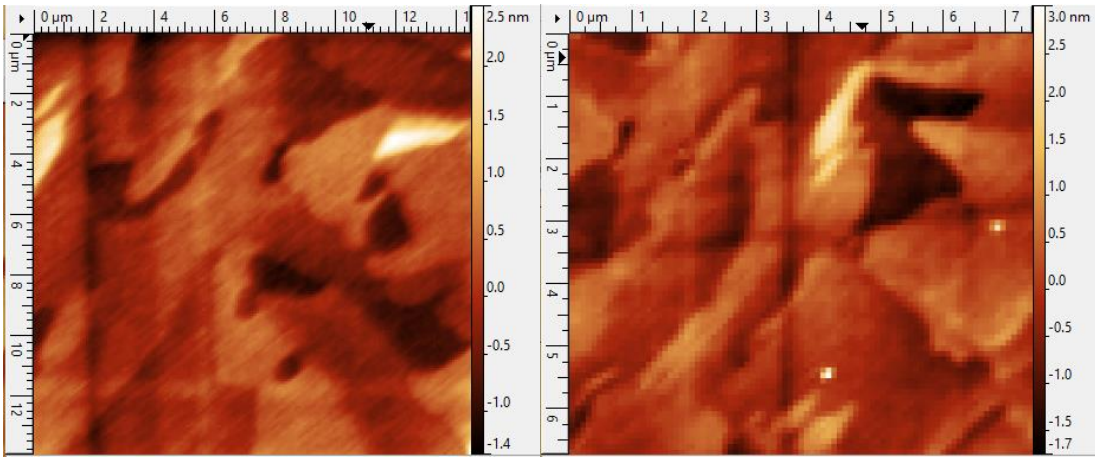

Figure 5.8 – An enlarged image of the exposed region of BSSCO on day 1 (left) compared to the exposed region of BSSCO on day 145 (right).

Both images in Figure 5.8 look very similar, and along with their similar RMS roughness value calculated by Gwyddion, it was concluded that the surface roughness does not significantly change within the observation period of 145 days. BSSCO does not oxidate at the same rate as TiS_2 due to its chemical composition, leading to a less drastic change in surface roughness in general.

Chapter 6. Conclusions

This study was conducted to investigate how carbon nanoparticles in layered materials change over time. Carbon nanoparticles move and diffuse over time within layered materials after initial intercalation as observed by Kidd et al. and others. Understanding this diffusion is important to understand the stability of the nanoparticles within different layered materials.

The increase in height in the TiS_2 sample shows that significant material is stored within the layers, and this material diffuses upwards. Increase in overall peak height and area with time shows that embedded nanoparticles diffuse from the bulk upwards. Increase in the distance of peak position with time from the center also indicates lateral diffusion. However, height increases by a factor of 463.3% and lateral position by 91.48% with time which shows most of the diffusion is in the vertical direction. Surface roughness increases on the exposed region and on the background region. There are two processes that cause the surface roughness to increase. On the exposed region, it was observed that nanoparticles at the surface move and aggregate to create piles of material on the surface. The height of these piles increases with time as more material aggregates, increasing the RMS recorded on the exposed region. On the background region, oxidation causes small surface roughness changes over time. Both processes cause the surface roughness on both regions to increase at similar rates. The relationship between these two processes is unknown and could be further explored in a future study.

The profiles taken on the BSSCO sample showed little change over the course of 145 days. Surface roughness was also observed to remain relatively constant throughout the observation period. Because of this, it was concluded that significant diffusion of nanoparticles does not occur within the layers of BSSCO during the designated observation period.

Carbon nanoparticles within TiS_2 should not be used in the fabrication of devices as they move significantly in short periods of time. This study proved that nanoparticles intercalated into TiS_2 are unstable and should therefore not be used to create devices. However, nanoparticles intercalated into BSSCO were shown to be much more stable as minimal diffusion was observed over a period of 145 days. If nanoparticles intercalated into BSSCO are shown to be stable over long periods of time with further observation, it would be a good choice for nanoscale devices.

Observation of these materials was limited by the amount of data taken in 2015. To further understand the diffusion of these carbon nanoparticles intercalated in the layered materials, more data points could be taken within the initial period of observation and beyond this period. Data collection could be automated in future to ensure more consistent data records. X-ray diffraction could also be utilized to monitor the spacing between layers over time. This could provide further insight into the movement of material within the layers.

This work is important in gaining a better understanding of the overall stability of these structures within layered materials. By understanding how material diffuses along and through the layers, information about the material can be learned. For example, observing the diffusion of carbon nanoparticles in BSCCO, a superconductor, parallels how an insulator would behave in BSCCO. The alternating superconductor and insulator can create Josephson tunnel junctions, which create qubits. Qubits are used in quantum computers to store data more efficiently.

References and Acknowledgements

Jung, Y., Zhou, Y., & Cha, J. J. (2016). Intercalation in two-dimensional transition metal chalcogenides. *Inorganic Chemistry Frontiers*, *3*(4), 452–463. https://doi.org/10.1039/C5QI00242G

Kidd, T. E., O'Shea, A., Beck, B., He, R., Delaney, C., Shand, P. M., Strauss, L. H., Stollenwerk, A., Hurley, N., Spurgeon, K., & Gu, G. (2014). Universal Method for Creating Optically Active Nanostructures on Layered Materials. *Langmuir*, *30*(20), 5939–5945. https://doi.org/10.1021/la501013x

Krasheninnikov, A. V., & Nordlund, K. (2010). Ion and electron irradiation-induced effects in nanostructured materials. *Journal of Applied Physics*, *107*(7), 071301. https://doi.org/10.1063/1.3318261

Lv, R., Robinson, J. A., Schaak, R. E., Sun, D., Sun, Y., Mallouk, T. E., & Terrones, M. (2015). Transition Metal Dichalcogenides and Beyond: Synthesis, Properties, and Applications of Single- and Few-Layer Nanosheets. *Accounts of Chemical Research*, *48*(1), 56–64. https://doi.org/10.1021/ar5002846

Nanofabrication: Fundamentals And Applications. (n.d.). Retrieved April 1, 2023, from https://web.s.ebscohost.com/ehost/ebookviewer/ebook/ZTAwMHhuYV9fMjM2MDk2X19BTg2?sid=ea395244-0936-4901-8990-76d8dc67d044@redis&vid=0&format=EB&lpid=lp_341&rid=0

Nečas D., Klapetek P., Gwyddion: an open-source software for SPM data analysis, *Cent. Eur. J. Phys.* 10(1) (2012) 181-188

Pimpin, A., & Srituravanich, W. (2012). Review on Micro- and Nanolithography Techniques and Their Applications. *Engineering Journal*, *16*, 37–56. https://doi.org/10.4186/ej.2012.16.1.37

Rykaczewski, K., Marshall, A., White, W. B., & Fedorov, A. G. (2008). Dynamic growth of carbon nanopillars and microrings in electron beam induced dissociation of residual hydrocarbons. *Ultramicroscopy*, *108*(9), 989–992. https://doi.org/10.1016/j.ultramic.2008.04.006

Rykaczewski, K., White, W. B., & Fedorov, A. G. (2007). Analysis of electron beam induced deposition (EBID) of residual hydrocarbons in electron microscopy. *Journal of Applied Physics*, *101*(5), 054307. https://doi.org/10.1063/1.2437065

Scientific Image—Atomic Force Microscope Illustration | NISE Network. (n.d.). Retrieved April 25, 2023, from https://www.nisenet.org/catalog/scientific-image-atomic-force-microscope-illustration

Stollenwerk, A. J., Hurley, N., Beck, B., Spurgeon, K., Kidd, T. E., & Gu, G. (2015). Manipulation of subsurface carbon nanoparticles in Bi 2 Sr 2 CaCu 2 O 8 + δ using a scanning tunneling microscope. *Physical Review B*, *91*(12), 125425. https://doi.org/10.1103/PhysRevB.91.125425

Transition metal dichalcogenide monolayers. (2023). In *Wikipedia*. https://en.wikipedia.org/w/index.php?title=Transition_metal_dichalcogenide_monolayers&oldid=1140219150

Zhang, J., Yang, A., Wu, X., van de Groep, J., Tang, P., Li, S., Liu, B., Shi, F., Wan, J., Li, Q., Sun, Y., Lu, Z., Zheng, X., Zhou, G., Wu, C.-L., Zhang, S.-C., Brongersma, M. L., Li, J., & Cui, Y. (2018). Reversible and selective ion intercalation through the top surface of few-layer MoS2. *Nature Communications*, *9*, 5289. https://doi.org/10.1038/s41467-018-07710-z

I would like to acknowledge Dr. Tim Kidd for all his help throughout this project. I could not have made it this far without him!

I would like to acknowledge Dr. Jessica Moon and the UNI Honors Program for their support through this process as well as throughout the past four years.

I would also like to thank the UNI Physics Department and my friends and family!

This work is supported by Grant No. DE-SC0020334 funded by the US Department of Energy, Office of Science, and the Nadyne Harris Scholarship for Honors Research from the University Honors Program.